Laser and Particle Beams (2000), *18*, 467–475. Printed in the USA.

Beyond the moving mirror model: Attosecond pulses from a relativistically moving plasma

L. ROSO,[1] L. PLAJA,[2] K. RZĄŻEWSKI,[3] AND D. VON DER LINDE[4]

[1]Departamento de Fìsica Aplicada, Universidad de Salamanca, E-37008 Salamanca, Spain
[2]Fakultät für Physik, Universität Bielefeld D-33501 Bielefeld, Germany
[3]Center for Theoretical Physics and College of Science, Polish Academy of Sciences, Aleja Lotników 32/46, 02-668 Warsaw, Poland
[4]Institute für Laser- und Plasmaphysik, Universität Essen D-45117 Essen, Germany

(RECEIVED 21 July 1999; ACCEPTED 31 October 1999)

Abstract

A simple model is proposed to study the field generated by a 3D plasma layer. The model neglects electron–electron interactions in the same way as occurs in the well known moving mirror models. However, the present model considers the radiation emitted by the moving electrons in a more precise way than in the mirror models, and allows the study of underdense or near critical plasmas. Results, including the transverse intensity profile of the driving field, are presented that show the possibility of generating trains of attosecond pulses.

1. INTRODUCTION

Numerical simulation of the interaction of a very intense laser beam with a plasma target implies the use of sophisticated computed codes due to the presence of multiple interacting electric charges. For terawatt laser pulses lasting only a few femtoseconds, the state of the art in those simulations are the so called *particle-in-cell* codes (Dawson, 1983; Kruer, 1988; Birdsall & Langdon, 1991; Gibbon, 1996; Pukhov & Meyer-ter-Vehn, 1996). Those codes consider groups (cells) of electrons moving at once. Of course, the ultimate goal would be to describe each individual electron separately, but this is beyond the capabilities of today's computers and it is doubtful that this has physical sense. *Particle-in-cell* codes with a 1D array of cells are feasible with current computers. 2D arrays, under certain approximations, seem feasible but time consuming and 3D *particle-in-cell* simulations are restricted to simple cases. In the fully relativistic case, that is, when the Liénard Wiechert correction is fundamental, as has been shown in a recent paper by Plaja and Conejero Jarque (1998) using a 1D model. Extension of fully relativistic *particle-in-cell* codes to 2 or 3D simulations seems to be very complicated due to the anisotropy of the generated field, and in most of the cases the simulations are restricted to include just retardation in an approximated way.

Address correspondence and reprint requests to: Luis Roso, Grupo de Optica, Departamento de Fisica Aplicada, Universidad de Salamanca, Plaza de la Merced, S/N 37008 Salamanca, Spain. E-mail: roso@gugu.usal.es

Therefore it seems useful to generate intermediate models to understand the physical phenomenology arising from the 3D nature of the problem. It is worth trying to describe the underlying physics of a plasma interacting with a very intense laser field in a way, maybe not as realistic, but certainly not as complicated as are the *particle-in-cell* codes. A model developed in this context is the so-called moving mirror model, or oscillating mirror model (Bulanov, *et al.*, 1994; Lichters, *et al.*, 1996; von der Linde & Rzążewski, 1996). Mirror models consider the electron plasma as a mirror that is driven by the laser field and by a restoring force, typically harmonic, due to the positive ions.

Perhaps the most interesting application of these simple models is the understanding of the basic features of the plasma dynamics that lead to surprising properties of the generated fields. Particularly relevant seems to be the possibility that phase-locked high order harmonics of the incoming laser field appear. By Fourier transforming from frequency to time domain it is straightforward to show that phase-locked harmonics combine into a train of short pulses. The duration of each individual pulse gets smaller as the number of harmonics generated increases. It is widely accepted today that there are several techniques that seem to be good candidates for the generation of extremely short pulses, subfemtosecond, but the studied proposal using a thin plasma slab and not requiring a filtering of the first components seems to be very promising (Plaja, *et al.*, 1998)

The aim of this paper is to propose a new approximated model to describe the driven plasma based on the indepen-

dent motion of each electron of the plasma. The model goes one step beyond the moving mirror models, in the sense that is able to give information on overdense as well as underdense or near critical plasmas, situations where most of the light is transmitted and the idea of having a mirror, with the total electric field vanishing at its surface, loses its sense.

After this introduction, the paper is organized in two parts. Section 2 gives an outline of the basic ideas needed on fields, moving charges, radiated fields and relativistic mirrors. Section 2.1 is used to describe the model for the laser and, particularly, for the plasma. Restoring force acting on the electrons is introduced in this section, together with a discussion of its validity in the relativistic domain. Section 2.2 is devoted to the study of the fields generated by the moving charges, using the well known expressions for the radiated field. Section 2.3 reviews the moving mirror model, with the condition of vanishing field at the mirror surface properly stated in the strongly relativistic regime. Section 3 is devoted to the presentation of the new model based on independently moving electrons. Section 3.1 studies the plane wave situation, fully neglecting the transverse structure of the field. This study is comparable to other existing models (Plaja, *et al.*, 1998), and allows a deep understanding of the physical mechanisms leading to the generation of very short pulses. Section 3.2 describes the influence of the transverse structure just at the waist of the focalized beam. Finally, Section 3.3 discusses the applicability of the model out of the waist, introducing a quadratic phase in addition to the transverse intensity profile. The paper ends with a final section devoted to conclusions.

2. FIELDS, CHARGES AND MIRRORS

2.1. Fields acting on the charges

We consider a Gaussian TEMoo mode, as schematically indicated in Figure 1, in paraxial approximation, trying to describe the transverse shape and the phase relations. It is a reasonable approximation to consider then the electric field **E** is linearly polarized along the *y*-axis, neglecting the other two components (we will always work in the paraxial limit). Then the incoming electric field is given by

$$E_y(x,y,z,t) = A\,\frac{w_0}{w(x)}\exp\left(-\frac{(x-ct)^2}{\tau^2}\right)\exp\left(-\frac{y^2+z^2}{w^2(x)}\right)$$

$$\times\exp\left[ik\left(x+\frac{y^2+z^2}{2R(x)}\right)\right]\exp(-i\omega t). \qquad (1)$$

The Guoy phase shift has been neglected, because we consider plasma slabs with longitudinal widths much smaller than the Rayleigh range. The transverse intensity profile is, $w(x) = w_o(x_o^2+x^2)^{1/2}/x_o$, and the transverse phase (convergent and divergent part of the beam) is given by, $R(x) = (x_o^2+x^2)/x$.

In the present paper we will compare the well-known plane wave approach, the only possibility for the moment when working with *particle-in-cell* codes and strongly relativistic dynamics, with results for a transverse distribution of the field. We will restrict ourselves to the waist of the beam because this is the point where the maximum intensity is reached.

On the other hand, the dynamics of the electron due to this incoming field is given by the well known Lorentz force. However, we have also to introduce the effect of the positive ions. To do this it is possible to assume that restoring force is harmonic with a resonant plasma frequency ω_P. Observe that the introduction of such plasma frequency in the strongly relativistic domain is just an approximation. The typical model of restoring force due to the positive ions is a nonrelativistic model and thus it has to be corrected in our case. The oscillation frequency in the relativistic case is not exactly the plasma frequency due to the difference between the rest mass, m, and the relativistic mass, $m\gamma$, of the moving electron, $\gamma = 1/\sqrt{1-v^2/c^2}$ being the standard relativistic factor for a motion with velocity v (c stands for the speed of light). It is the authors opinion that working more deeply in the meaning of such a relativistic harmonic oscillator is just an academic problem. 1D *particle-in-cell* simulations indicate that a restoring force appears and show that for a certain range of the electron cloud excursion, the force can be considered as harmonic. However, for large excursions of the electrons away from the ions, restoring force begins to look more like a capacitor force (linear potential) than an harmonic oscillator (quadratic potential).

In the model developed in the present paper, relativistic dynamics of the electron driven by the Lorentz and the restoring forces will be given by

$$\frac{d\mathbf{p}}{dt} = q\mathbf{E}(\mathbf{r},t) + \frac{q}{c}\,\mathbf{v}\wedge\mathbf{B}(\mathbf{r},t) - m\omega_P^2(x-x_0)\mathbf{e_x}. \qquad (2)$$

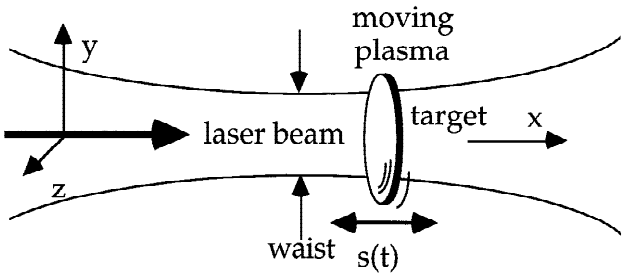

Fig. 1. Geometry described in the present paper: a Gaussian TEMoo laser pulse interacting with a flat and very thin plasma target. The target reflects part of the incoming light if the plasma is underdense or acts as a total mirror if the plasma is overdense. For simplicity we consider that the electric field is polarized along the *y* axis, and the magnetic field lies along the *z* axis, being *x* the propagation direction.

https://doi.org/10.1017/S0263034600183168 Published online by Cambridge University Press

At this point it is convenient to introduce the relativistic velocity, $\mathbf{u} = \gamma\mathbf{v}$. Thus, $\gamma = \sqrt{1+u^2/c^2}$, and

$$\frac{d\mathbf{u}}{dt} = \frac{q}{m}\,\mathbf{E}(\mathbf{r},t) + \frac{q}{\gamma mc}\,\mathbf{u}\wedge\mathbf{B}(\mathbf{r},t) - \omega_P^2(x-x_0)\mathbf{e_x}. \qquad (3)$$

Individual pairs of interacting electrons are not considered. So the present model is much simpler than a *particle-in-cell* code. Also the influence of the field generated by one electron on the other electrons is neglected.

In coordinates,

$$\begin{cases} \dfrac{du_x}{dt} = \dfrac{q}{\gamma mc}\,u_y B_z(x,t) - \omega_P^2(x-x_0) \\ \dfrac{du_y}{dt} = \dfrac{q}{m}\,E_y(x,t) - \dfrac{q}{\gamma mc}\,u_x B_z(x,t) \end{cases}. \qquad (4)$$

Due to the geometry of this problem, with a linearly polarized laser field, the electron's motion is restricted to the *xy* plane (the electron is initially at rest). Most of the new and interesting dynamics of these models lies in the fact that the relativistically driven harmonic oscillator presents a nice nonlinearity due to the change of mass as the velocity increases. It has been recently shown (Kim & Lee, 1995; Lee *et al.*, 1997) that this system is chaotic for certain ranges of parameters. The scope of the paper is not in this dynamical behavior but to use this strong nonlinear motion to tailor the time profile of the reflected field.

Figure 2 shows the velocity for three different trajectories of the speed that involve very different restoring forces. The driving laser frequency is equal to $\omega_L = 0.055$ a.u., that corresponds to a wavelength in free space $\lambda = 800$ nm. To reach the strongly relativistic regime we have considered an electric field amplitude $E_0 = 25$ a.u., that is, an intensity $I = 2.2\ 10^{19}$ W/cm^2. The effect of the plasma density, through the restoring force, is studied for three different values. Figure 2a shows the motion for the case of an overdense plasma, $n = 10n_c$, n_c being the critical density, that is, the density at which the plasma frequency equals the incoming laser frequency. Therefore $n = 10n_c$ corresponds to a plasma frequency $\omega_P = 0.17$ a.u. $= \sqrt{10}\omega_L$. In this case, restoring force dominates the motion introducing two competing frequencies, plasma and laser, that lead to irregular dynamics not very adequate for the generation of short pulses. Figure 2b shows the motion for the case of a critical density plasma, $n = n_c$, that corresponds to a plasma frequency $\omega_P = 0.055$ a.u. Finally, Figure 2c shows the motion for the case of an underdense plasma, $n = 0.1n_c$, that corresponds to a plasma frequency $\omega_P = 0.017$ a.u. The two last cases show remarkably similar and regular dynamics. Observe that the driving laser has a Gaussian time profile $\exp(-t^2/\tau^2)$, with a duration equal to twenty cycles, $\tau = 10 \times 2\pi/\omega_L$. In the first case, dynamics during turn-on and turn-off are very different while in the two other cases trajectories are reversible.

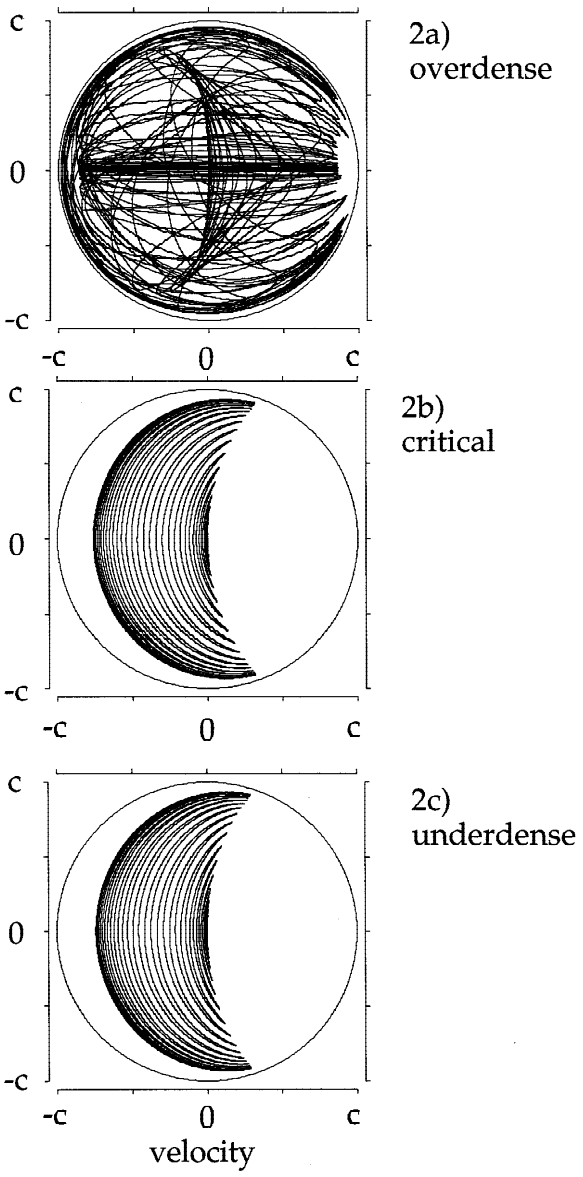

Fig. 2. Relativistic velocity corresponding to three different electronic trajectories driven by a laser field of intensity $I = 2.2\ 10^{19}$ W/cm^2 (electric field amplitude $E = 25$ a.u.) and frequency $\omega_L = 0.055$ a.u. (that corresponds to a wavelength of approximately 800 nm). The laser pulse has a Gaussian time profile with a width equal to 20 cycles. Figure 2a corresponds to the overdense regime ($n = 10\ n_c$). Figure 2b is just for the critical density ($n = n_c$). Figure 2c corresponds to an underdense plasma ($n = 0.1\ n_c$).

2.2. Charges acting on fields

Once the dynamics of a single electron is understood, it is necessary to compute the field generated by those charges. The reflected far field (exactly backwards) is given by,

$$E_y(x,t) = e\left[\frac{ca_y - v_x a_y + v_y a_x}{R(c+v_x)^3}\right]_{ret}, \qquad (5)$$

R is the distance from the charge to the point where the electric field is evaluated. Of course, retardation has to be in-

https://doi.org/10.1017/S0263034600183168 Published online by Cambridge University Press

cluded. In these expressions the electrons are driven only by the incident field, not by the field generated by the other electrons (another difference with a particle-in-cell code).

This point introduces the main difference with the existing moving mirror models. In such models the electric field vanishes at the mirror surface (in the mirror rest frame) as it is going to be reviewed in the next section. Thus reflection happens at all times, but oscillating Doppler effect enhances it at certain times and reduces it in other parts of the oscillation. Computation of the field generation from the more accurate expression for the far field introduced at the beginning of the present section indicates that the denominator originates an enhancement of this nonlinear behavior, so the peaks are more pronounced and there is a flat region with a very small emitted field.

A typical schematic trajectory of the relativistically driven electron with a critical restoring force is shown in Figure 3. We prefer to show a scheme instead of the draw of a real trajectory because the motion is not fully regular. Trajectories are not totally periodic and show a drift and other irregularities due to the nonlinear behavior induced through the quadratic denominator inside the relativistic factor γ. As indicated in Figure 2a for the velocities, this nonlinearity is more evident in the overdense case and it is reasonably small for near critical and for underdense plasmas. This figure of eight motion in the laboratory frame has little in common with the well known figure of eight motion of a free electron (driven by intense laser fields) in the average rest frame.

Related to the generation of fields, Figure 3 gives a clear idea of possible directions of generation of scattered radiation. It is well known that in the strongly relativistic regime, light is generated essentially along the direction of motion of the electron. Therefore the field can not be generated in the forward direction (forward in the sense of the incoming intense field) because electrons never move along the positive x-axis. There are, however, two portions of the trajectory where electrons move backwards along this axis: these two correspond to the upper and lower parts of the figure of eight. In one driving laser cycle the whole figure of eight is drawn, therefore there are two moments where an intense field is scattered backwards. Because these two portions of the trajectory correspond to just opposite accelerations, the generated electric fields will have opposite signs. This will be the key point to give a physical insight of the generation of attosecond pulses. We will come back to these ideas later on.

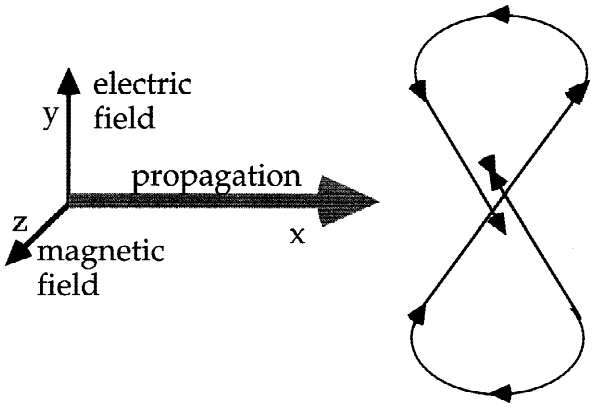

Fig. 3. Schematic representation of a typical figure of eight trajectory of the relativistic driven harmonic oscillator (close to critical).

2.3. Totally reflecting mirror

The standard definition of a totally reflecting mirror is given through the condition of a vanishing electric field ($E_{total} = 0$). But this condition needs to be used with care. The condition is valid in a frame where the electron is at rest, therefore we have to convert the field from the laboratory frame to a frame moving at the speed of the mirror.

If $E_y(x,t)$ and $B_z(x,t)$ are the electric and magnetic fields, respectively, in the laboratory frame, then in the mirror frame the electric field is given by,

$$E'_y(x,t) = \gamma\left(E_y(x,t) + \frac{v}{c}B_z(x,t)\right) = 0. \tag{6}$$

Because the electric and magnetic fields have a forward component (+) and a backward component (−), they can be written in the form,

$$\begin{aligned} E_y(x,t) &= +E^+(t-x/c) + E^-(t+x/c) \\ B_z(x,t) &= -E^+(t-x/c) + E^-(t+x/c). \end{aligned} \tag{7}$$

The condition of vanishing field at the mirror becomes,

$$E^-(t+s(t)/c) = -\frac{1-v(t)/c}{1+v(t)/c}E^+(t-s(t)/c). \tag{8}$$

A solution of this expression also shows the trains of attosecond pulses we are looking for, but with a slightly different time profile of the pedestals (Plaja *et al.*, 1998) between consecutive peaks. One difference of the moving mirror results with the *particle-in-cell* computations is due to the fact that here the field is reflected backwards at all times. In a more realistic model the reflected field is generated only at specific moments of the electron trajectory.

Working with a single frequency field and an overdense plasma we could consider that the mirror model is essentially correct. However, for attosecond pulses, generation high order harmonics is implied. It is possible that the plasma acts as a perfect mirror for the incoming laser but not for the high harmonics. This is, of course, well accounted for in the *particle-in-cell* simulations.

3. PARTIALLY REFLECTING MIRROR

In this part we try to present a new model based on the motion of independent electrons. This model is able to describe the reflected field in cases when the plasma is overdense and

https://doi.org/10.1017/S0263034600183168 Published online by Cambridge University Press

also when the plasma is underdense. Electrons are driven by the laser field and by a restoring harmonic force (at the plasma frequency), and dynamics can be studied as the laser frequency is tuned from one side to the other of the resonance.

3.1. Plane wave model

Neglecting all transverse effects, one obtains a plane wave model. This model improves the moving mirror, in the sense that it is full relativistic (but has the same difficulties in order to account for the beam transverse intensity profile).

Several typical results for this case are shown in Figure 4. Figure 4a represents the time profile of the reflected electric field for a driving laser of intensity $I = 2.2\ 10^{19}$ W/cm^2 (corresponding to an electric field amplitude $E = 25$ a.u.) and frequency $\omega_L = 0.055$ a.u. (that corresponds to a wavelength of 800 nm). The laser pulse is a plane wave in space and is linearly turned on during four cycles and then it is constant in time. The plasma layer thickness is equal to $\lambda/20$ (i.e., 40 nm). The plasma frequency is equal to the laser frequency, $\omega_P = 0.055$ a.u. (critical density). Due to the figure of eight motion of the relativistically driven electrons, the backward scattered field is no longer sinusoidal but has a structure with sharp spikes. Therefore a train of attosecond pulses is obtained. Pulses are not completely regular due to the non strictly-periodic electronic trajectories, and the delay between two consecutive peaks is not exactly equal to the laser period.

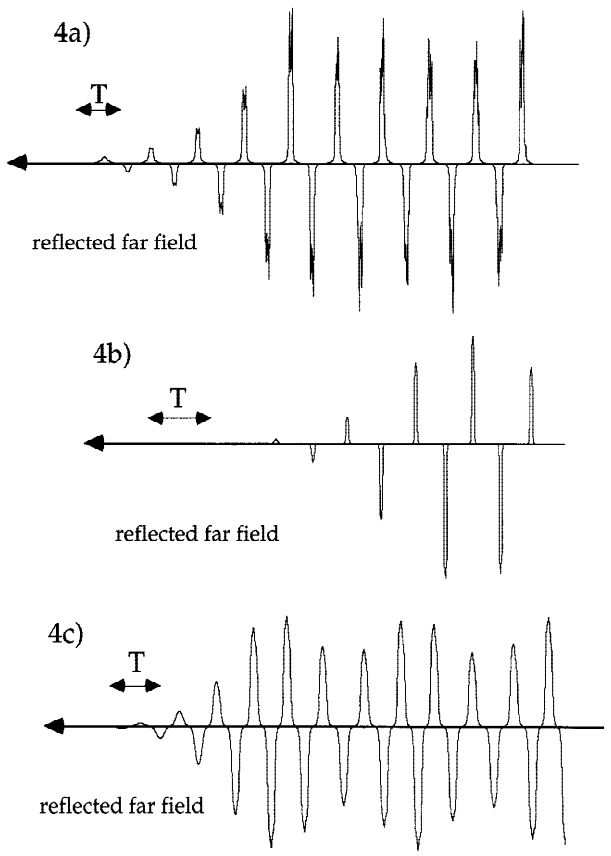

Fig. 4. Time profile of the reflected electric field for different parameters but always in the plane wave model, that is, with a constant transverse intensity profile. The laser pulse is a plane wave in space and is linearly turned on during four cycles and then it is constant in time. Figure 4a corresponds to a laser of intensity $I = 2.2\ 10^{19}$ W/cm^2 (electric field amplitude $E = 25$ a.u.) and frequency $\omega_L = 0.055$ a.u. (800 nm wavelength). The plasma layer thickness is equal to $\lambda/20$ (i.e., 40 nm). The plasma frequency is equal to the laser frequency, $\omega_P = 0.055$ a.u. (critical density). Figure 4b corresponds to the same field but to a thinner plasma layer (only $\lambda/50$, that is 16 nm), and undercritical, $\omega_P = 0.017$ a.u. Figure 4c corresponds to an intensity $I = 3.5\ 10^{18}$ W/cm^2 (electric field amplitude $E = 10$ a.u.) and frequency $\omega_L = 0.055$ a.u. (800 nm wavelength), and a plasma layer of thickness $\lambda/10$ and underdense, $\omega_P = 0.017$ a.u. The horizontal arrows indicate the laser period, $T = 2\pi/\omega_L$. Vertical scale gives the reflected electric field in arbitrary units.

Figure 4b corresponds to a thinner plasma layer (only $\lambda/50$, that is 16 nm), and undercritical, $\omega_P = 0.017$ a.u. (that corresponds to a density 10 times smaller than the critical density). In this case—with a bit unrealistic parameters—the structure of the attosecond peaks seems more clear. To our knowledge, the shape of the peaks depends on two factors. First, the relativistic trajectory has to be quasi regular. Second, the plasma thickness influences the relative phases of the light scattered back at each plane, and the width of each peak increases with the thickness. The width of the peaks is proportional to d/c (d being the thickness of the plasma layer), as long as it is smaller than half of the optical period.

Just for comparison, a case where the reflected wave looks sinusoidal is included in Figure 4c. It corresponds to an intensity $I = 3.5\ 10^{18}$ W/cm^2 (corresponding to an electric field amplitude $E = 10$ a.u.) and a frequency $\omega_L = 0.055$ a.u. (a wavelength of 800 nm). The plasma layer, of thickness $\lambda/10$, is underdense, with $\omega_P = 0.017$ a.u. (that corresponds to a density 10 times smaller than the critical density). The laser frequency and intensity are chosen so that the electron motion becomes slightly relativistic and the radiated field begins to show the signature of the trains of short pulses.

The problem with all these results is that a plane wave model does not take into account the transverse profile. Electrons at different parts of the target will experience fields with different amplitude (and phase—if out of the waist). Therefore we would like to know the influence of a transverse profile.

3.2. Transverse profile at the waist

Assume that the plasma slab is located just at the waist of the laser beam, and assume that the target is much thinner than the wavelength (otherwise attosecond peaks will not appear). This model takes into account the coherent sum of the fields generated by electrons at different positions (electrons that feel different laser intensities). Assume that the target is located just at the waist of the laser beam (only a transverse distribution of amplitudes and not of phases), and assume that the target is much thinner than the wavelength.

https://doi.org/10.1017/S0263034600183168 Published online by Cambridge University Press

The incoming field is a plane wavefront (yz-plane), therefore to study the reflected field we can consider a parallel plane wavefront. To compute the reflected field we need to compute the field $E_y(x_0, y_0, z_0, t)$, for a very large value of x_0 (far field), and for the transverse coordinates y_0, z_0, equal to the coordinates of the considered electron. We need to compute emission just along the x-axis. Then all those fields can be simply added (as amplitudes) to get the output. Thus the reflected field at each point is added in a way that corresponds to focus the far field at $x \to -\infty$.

Each point of the target is driven by a laser field of amplitude proportional to, $\exp[-(y^2 + z^2)/w_0^2]$. If the transverse profile is changing slowly (large w_0, compared with the wavelength) then the introduction of this transverse structure is like an integral of different concentric rings, each one comparable to the case studied in Section 3.1.

When adding (coherently) the contributions of all those points, adding electrons that feel different laser intensities, we find a reflected field profile showing the same trains of attosecond pulses.

The field generated by each individual electron, i, is given by

$$E_y^i(x,t) = e\,\frac{ca_y^i - v_x^i a_y^i + v_y^i a_x^i}{R(c+v_x^i)^3}\Big]_{ret} \tag{9}$$

R being the distance to the wavefront, that is, the distance along the x-axis (y and z being constant). Summation for all charges in the target gives,

$$E_y(x,t) = \sum_i \frac{ca_y^i - v_x^i a_y^i + v_y^i a_x^i}{R(c+v_x^i)^3}\Big]_{ret}, \tag{10}$$

the index i indicates the different point charges in the target. In other words, this is equivalent to consider only fields in the x direction and consider charges that—being at the same point—feel different laser intensities, and then adding all the fields.

Results for this case with a beam waist equal to 10 wavelengths is shown in Figures 5 and 6 for different choices of the parameters, also showing the robustness of the present model. Figure 5 illustrates the dependence with the plasma density. It corresponds to the case of a Gaussian transverse intensity profile $\exp[-(y^2+z^2)/(10\lambda)^2]$ (waist equal to 20 wavelengths) and without relative phases (plasma target just at the waist of the laser beam). These drawings correspond to an intensity $I = 2.2\ 10^{19}$ W/cm^2 (electric field amplitude $E = 25$ a.u.) and a frequency $\omega_L = 0.055$ a.u. (wavelength $\lambda = 800$ nm). The field amplitude increases with a turn on of 6 cycles and it is then constant. The plasma layer thickness is $\lambda/5$ is a bit too big to obtain nice attosecond peaks, but it is very convenient to check the effects of the plasma density. The three drawings correspond to three different values of the plasma density. Figure 5a corresponds to an underdense plasma $n = 0.1\ n_c$ (plasma frequency $\omega_P = 0.017$ a.u.). In this figure only one or two nice peaks appear (the rest is averaged by the plasma thickness and by the space intensity profile). Figure 5b corresponds to a plasma with just the critical density $n = n_c$ (plasma frequency $\omega_P = 0.055$ a.u. = ω_L equal to laser frequency). Finally, Figure 5c corresponds to a overdense plasma $n = 10\ n_c$ (plasma frequency $\omega_P =$ 0.17 a.u.). All cases evidence the need of thinner plasma layers, as presented in Figure 6. Figure 6a corresponds exactly to the same parameters as Figure 5b (plasma with just the critical density $n = n_c$) but with a plasma layer equal to $\lambda/20$. Figure 6b to a layer of only $\lambda/50$. The influence of the thickness of the plasma layers seems fundamental for the generation of trains of short pulses.

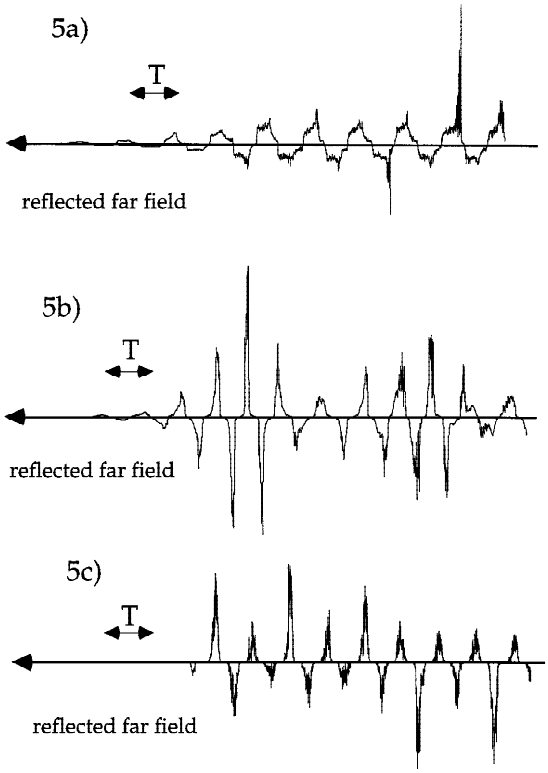

Fig. 5. Time profile of the reflected electric field for the case of a Gaussian transverse intensity profile $\exp[-(y^2 + z^2)/(10\ \lambda)^2]$ (waist equal to 20 wavelengths) and without relative phases (plasma target just at the waist of the laser beam). These drawings correspond to an intensity $I = 2.2\ 10^{19}$ W/cm^2 (electric field amplitude $E = 25$ a.u.) and a frequency $\omega_L = 0.055$ a.u. (wavelength $\lambda = 800$ *nm*). The field amplitude increases with a turn on of six cycles and it is then constant. The plasma layer thickness is $\lambda/5$. The three drawings correspond to three different values of the plasma density. Figure 5a corresponds to an underdense plasma $n = 0.1\ n_c$ (plasma frequency $\omega_P = 0.017$ a.u.). Figure 5b corresponds to a plasma with just the critical density $n = n_c$ (plasma frequency $\omega_P = 0.055$ a.u. = ω_L equal to laser frequency). Finally, Figure 5c corresponds to a overdense plasma $n = 10\ n_c$ (plasma frequency $\omega_P = 0.17$ a.u.). The horizontal arrows indicate the laser period, $T = 2\pi/\omega_L$. The vertical scale gives the reflected electric field in arbitrary units.

Since the appearance of the trains of attosecond peaks requires a very high intensity, it is necessary to focus the beam over a very small spot. As a general conclusion we have observed that the beam profile can be taken into account and the attos profile still remains on.

https://doi.org/10.1017/S0263034600183168 Published online by Cambridge University Press

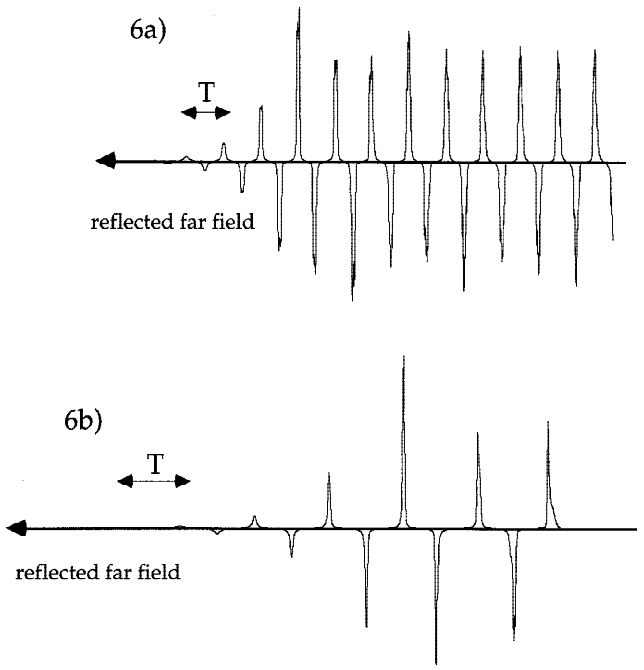

Fig. 6. Time profile of the reflected electric field for the case of a Gaussian transverse intensity profile $\exp[-(y^2 + z^2)/(10\ \lambda)^2]$ (waist equal to 20 wavelengths) and without relative phases (plasma target just at the waist of the laser beam). These drawings correspond to an incident laser intensity $I = 2.2\ 10^{19}$ W/cm^2 (electric field amplitude $E = 25$ a.u.) and a frequency $\omega_L = 0.055$ a.u. (wavelength $\lambda = 800\ nm$). The field amplitude increases with a turn on of six cycles and it is then constant. The figures correspond to a plasma with just the critical density $n = n_c$ (plasma frequency $\omega_P = 0.055$ a.u. $= \omega_L$ equal to laser frequency). These results show the influence of the plasma layer thickness. Figure 6a corresponds to a plasma layer equal to $\lambda/20$. Figure 6b to a layer of only $\lambda/50$. The horizontal arrows indicate the laser period, $T = 2\pi/\omega_L$. The vertical scale gives the reflected electric field in arbitrary units.

3.3. Description of a realistic beam focus profile

With the present model it is also possible to consider that the target is located before of after the beam waist. In this case it is necessary to introduce a dephasing (quadratic) from point to point, and the rest of the model is still valid. For the paraxial beam introduced at the beginning of the paper, this quadratic dephasing is given by $\exp[ik(y^2 + z^2)/2R(x)]$. Notice that it can be equivalently obtained with a spherical optical component in paraxial approximation. Of course, the transverse intensity profile, $\exp[-(y^2 + z^2)/w^2(x)]$ must also be taken into account.

In this case, we can consider that the target surface is divided in concentric circles (with center in the beam axis) and that each circle generates attosecond peaks with a given phase. The summation of all those attosecond peaks, in principle should be something like the summation with a shift (given by that phase). If the weight of each one is the same, then the result averages to zero. However, the weight of the phase at the y, z point depends on the area of this ring (as a surface differential). The larger is the radius the bigger is the contribution of this ring. As we pass the waist then the intensity drops and those outer rings come to be less important. This difference of weights causes that the averaging does not to fall to zero, instead it has a nice structure of broad peaks with a few very narrow ones that remain in certain cases. However, due to the dependence of the results of the rest of the parameters it does not seem convenient to include drawings on this.

In any case, if we are interested in collecting much of the light reflected at this partial mirror, we need to work at the geometrical image. In this case the phase difference introduced by the quadratic dephasing has to be compensated by an optical element. This means that we are in fact in a situation similar to Section 3.2. Even being out of the waist, the fields reflected at each point have to be added up—without additional phases—if working close to the geometrical image of a convenient optical system. Therefore the result of Section 6 is of general applicability.

4. CONCLUSIONS

A model consistent of independent fully relativistic moving charges is introduced to describe the interaction of a plasma with a very intense laser pulse. The influence of the positive ions is considered through a restoring force (harmonic oscillator). Results of the model go one step further than the well known moving mirror models, are relatively simple, and agree with the phenomenology observed in more elaborated simulations, as the *particle-in-cell* codes.

Previous published models to describe this experimentally feasible situation only considered plane wave beam profiles. The proposed model is able to give an insight on the effect of a transverse profile of the beam. The results of the model can not be considered qualitatively because electron–electron repulsion has been neglected.

The model gives additional indications that trains of very short pulses are expected to be found in the reflected light, even when working with a small focal spot and a transverse intensity profile. The parameters of intensity and frequency seem feasible with today's lasers, and many other relativistic effects have been already found in experiments. Probably the main problem, from the experimental point of view, to check the results proposed in this paper is the impossibility to detect such subfemtosecond time profile.

ACKNOWLEDGMENTS

Partial support from the Training and Mobility of Researchers Program of the European Commission (contract no CT96-0800), and from the Spanish Dirección General de Investigación Científica y Técnica (under contract PB95 0955), and from the Consejería de Educación y Cultura of the Junta de Castilla y León (Fondo Social Europeo), (under grant SA56/99) is acknowledged. K.R. thanks the Humboldt Foundation for its generous support. L.P. wishes to thank support from the Spanish Ministerio de Educación y Cultura (under grant EX98-35084508).

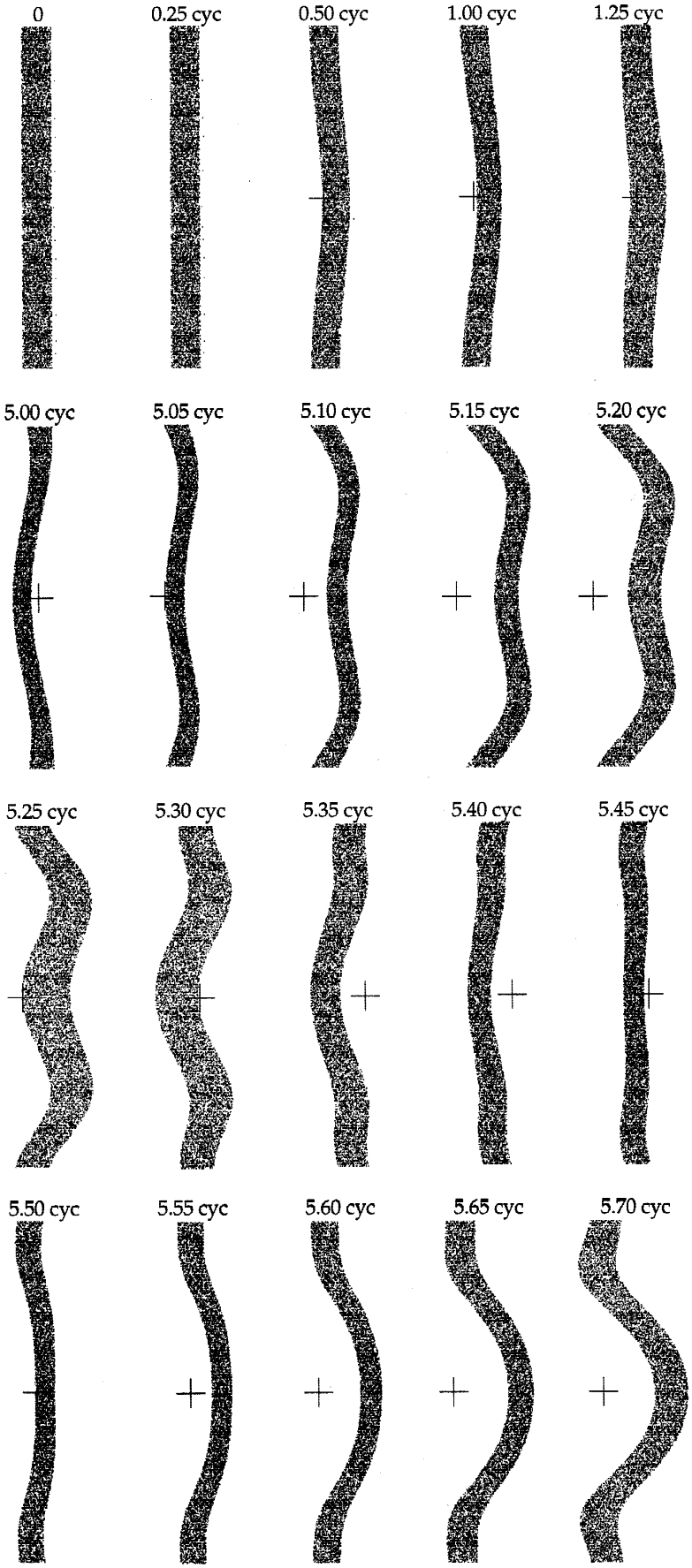

Fig. 7. Transverse profile of the plasma layer. Corresponds to the same parameters as the last drawing in Figure 4. To analyze the motion of the plasma layer the horizontal scale is enlarged 100 times. The scale is given by the central cross (centered at the waist): each horizontal arm length is equal to $\lambda/100$, each vertical arm length is equal to λ. Therefore, the initial thickness of the plasma layer is equal to $\lambda/50$.

https://doi.org/10.1017/S0263034600183168 Published online by Cambridge University Press

REFERENCES

Birdsall, C.K. & Langdon, A.B. (1991). *Plasma Physics via Computer Simulation, Plasma Physics Series*. Bristol: IOP Publishing.

Bulanov, S.V., Naumova, N.M. & Pegoraro, F. (1994). *Phys. Plasmas* **1**, 745.

Dawson, J.M. (1983). *Rev. Mod. Phys.* **55**, 403.

Gibbon, P. (1996). *Phys. Rev. Lett.* **76**, 50.

Kim, J.H. & Lee, H.W. (1995). *Phys Rev E* **51**, 1579.

Kruer, W.L. (1988). *The Physics of Laser Plasma Interactions.* New York: Addison Wesley.

Lee, S.W., Kim, J.H. & Lee, H.W. (1997). *Phys Rev E* **56**, 4090.

Lichters, R., Meyer-Ter-Vehn, J. & Pukhov, A. (1996). *Phys. Plasmas* **3**, 3425.

Plaja, L. & Conejero Jarque, E. (1998). *Phys Rev E* **58**, 3977.

Plaja, L., Roso, L., Rzążewski, K. & Lewenstein, M. (1998). *Jour. Opt Soc. Amer B* **15**, 1904.

Pukhov, A. & Meyer-Ter-Vehn, J. (1996). *Phys. Rev. Lett.* **76**, 3975.

Von Der Linde, D. & Rzążewski, K. (1996). *Applied Phys. B* **63**, 499.

https://doi.org/10.1017/S0263034600183168 Published online by Cambridge University Press